

Ab-initio Prediction of Conduction Band Spin Splitting in Zincblende Semiconductors

A. N. Chantis, Mark van Schilfgaarde and Takao Kotani¹

¹*Arizona State University, Tempe, Arizona, 85284, USA*

(Dated: January 24, 2018)

We use a recently developed self-consistent *GW* approximation to present systematic *ab initio* calculations of the conduction band spin splitting in III-V and II-V zincblende semiconductors. The spin orbit interaction is taken into account as a perturbation to the scalar relativistic hamiltonian. These are the first calculations of conduction band spin splittings based on a quasiparticle approach; and because the self-consistent *GW* scheme accurately reproduces the relevant band parameters, it is expected to be a reliable predictor of spin splittings. The results are compared to the few available experimental data and a previous calculation based on a model one-particle potential. We also briefly address the widely used $\mathbf{k}\cdot\mathbf{p}$ parameterization in the context of these results.

PACS numbers: 71.70.-d, 71.70.Ej, 71.15.-m, 71.15.Qe ,71.15.Mb)

In this letter, we apply a recently developed all-electron quasiparticle (QP) self-consistent *GW* method (QPsc*GW*) [1, 2, 3] to determine the spin splitting of conduction bands in III-V and II-VI zincblende semiconductors as a consequence of the spin-orbit coupling. This quantity is emerging as a parameter of great importance in spintronics applications, in part because it determines spin lifetimes, but also because it may be possible to exploit the splitting to induce spin current without an external magnetic field through the Rashba effect.

Information about this important quantity is very sparse. On the theoretical side, precise QP levels for the occupied and first few unoccupied states are required. We show here that QPsc*GW* accurately reproduces measured fundamental and higher-lying gaps in all the semiconductors studied, as well as other key parameters (effective mass, *d* band position, etc.), and is therefore a suitable vehicle for accurate determination of the splitting.

Owing to a lack of inversion symmetry, the conduction band of a zincblende semiconductor is split by spin-orbit coupling. Dresselhaus [4] showed that near the minimum point Γ_6^c , the splitting can be described by the operator $H_D = \frac{1}{2}\vec{\sigma} \cdot \vec{B}_{\text{eff}}$, where $\vec{\sigma}$ are the Pauli matrices and $B_{\text{eff}}^i = 2\gamma k_i(k_{i+1}^2 - k_{i+2}^2)$, $i = \{x, y, z\}$. H_D is written in this form to suggest that its effect is equivalent to the action of a \mathbf{k} -dependent effective magnetic field \vec{B}_{eff} , which is anisotropic in \mathbf{k} and is proportional to k^3 . γ is a constant that depends on the bulk properties of the material. Provided the Larmor precession frequency under $\vec{B}_{\text{eff}}(\mathbf{k})$ is less than the inverse of momentum relaxation time, small random changes in \mathbf{k} will cause the polarization of an injected current to gradually diminish. This is the spin scattering mechanism of Dyakonov and Perel (DP) [5]; and it is widely accepted that for a wide range of temperatures and moderate concentration of impurities, DP is the dominant spin relaxation mechanism in the conduction band of III-V and II-VI semiconductors. The DP spin scattering rate can be estimated theoretically once the value of γ is known [5].

In low dimensional structures the splitting scales in proportion to k , owing to confinement effects, which causes the DP mechanism to increase significantly. Moreover asymmetry in the leads or structure of a device results in an additional spin splitting effect, proposed first by Rashba and Bychkov [6]. This contribution from this “structural inversion asymmetry” depends on the boundary conditions: it can interfere constructively or destructively with the Dresselhaus term depending on device geometry and \mathbf{k} vector. Based on this, a few authors [7, 8, 9] proposed that growth of quantum wells in certain crystallographic directions can result in long spin coherence times, if the ratio of Dresselhaus to Rashba terms is close to unity. Measurements of these two contributions suggest that they can be comparable [10, 11]. Also giant spin relaxation anisotropy can occur in strained bulk zincblende semiconductors owing to destructive interference between the Dresselhaus and strain-induced spin splittings [8].

To evaluate γ theoretically, it is essential to use an *ab initio* approach rather than a parameterized method such as the $\mathbf{k}\cdot\mathbf{p}$ theory because the latter includes many external parameters whose values can only be reliably determined through fitting to an *ab initio* approach. However, the *ab initio* approach based on the usual local density approximation (LDA) is no better. This is because γ depends strongly on key features of the band structure, such as effective mass, that the LDA cannot reliably predict. As is well known, it is difficult to choose an appropriate empirical adjustment to the LDA potential so that the energy band structure of the lowest few conduction bands is reliable. This is particularly true in more complex cases such as quantum wells where experimental data is not available.

QPsc*GW* is a method to determine a (nonlocal but static) hermitian one-particle hamiltonian H_0 in a self-consistent way [1, 2]. With the usual *GW* approximation, we can calculate the self-energy $\Sigma(\omega)$ as a functional of the starting trial H_0 . Here $\Sigma(\omega)$ can be expanded in the basis of the eigenfunctions $\{\psi_{\mathbf{k}n}(\mathbf{r})\}$ of H_0 , where \mathbf{k} is

TABLE I: Important band parameters for the III-V semiconductors. E_0 and E'_0 are the energies of the first two conduction bands at the Γ -point, and are defined in the text; E_g is the fundamental gap when it differs from E_0 . m_c^Γ/m is the conduction band effective mass at Γ . Energies are in eV; γ is in eV·Å³. Quantities in rectangular brackets were computed from Eq. 2 with α chosen to reproduce the experimental fundamental gap E_g . Quantities in parenthesis and curly brackets correspond respectively to experimental data, and calculated data from Ref. 12. Spin orbit splittings Δ_{SO} and Δ'_{SO} do not change significantly whether the QPscGW, the scaled QPscGW or the LDA potential is used.

	AIP	AlAs	AlSb	GaP	GaAs	GaSb	InP	InAs	InSb
E_g	2.61	2.25	1.75	2.33					
(expt)	(2.51) ^a	(2.23) ^a	(1.69) ^a	(2.35) ^a					
E_0	4.52	3.33	2.66	3.00	1.80	1.16	1.56	0.68	0.54
(expt)	(3.63) ^a	(3.13) ^a	(2.38) ^a	(2.90) ^c	(1.52) ^a	(0.82) ^a	(1.42) ^a	(0.42) ^f	(0.24) ^a
$E'_0 - E_0$	1.46	2.13	1.22	1.98	2.81	2.10	3.32	3.10	2.69
[scaled Σ]					[2.89]	[2.26]	[3.34]	[3.78]	[2.82]
(expt)					(3.08) ^a	(2.37) ^a	(3.38) ^a		(2.91) ^a
Δ_{SO}	0.060	0.294	0.664	0.096	0.336	0.703	0.12	0.359	0.733
(expt)		(0.300) ^a	(0.673) ^a		(0.341) ^a	(0.756) ^a	(0.108) ^a	(0.371) ^g	(0.750) ^h
Δ'_{SO}	0.027	0.031	0.053	0.158	0.174	0.196	0.423	0.429	0.389
(expt)						(0.213) ^a	(0.070) ^a		(0.392) ^a
Δ^-	-0.10	-0.13	-0.32	+0.12	-0.12	-0.32	+0.21	+0.22	-0.29
{Ref. 12}					{-0.11}	{-0.32}	{+0.23}		{-0.24}
m_c^Γ/m	0.186	0.131	0.117	0.130	0.076	0.055	0.084	0.036	0.030
[scaled Σ]					[0.069]	[0.043]	[0.081]	[0.026]	[0.016]
(expt)					(0.067) ^a	(0.0412) ^a	(0.0765) ^a	(0.0231) ^a	(0.014) ^a
γ	+0.08	+3.4	+30.2	-2.3	+6.4	+81.8	-14.1	-27.8	+79.4
[scaled Σ]					[+8.5]	[+119.3]	[-15.7]	[-47.5]	[+209.6]
(expt)					(25.5) ⁱ	(186.2) ^j	(7.5-9.9) ^j		(+225±12) ^k
{Ref. 12}					{+14.9}	{+108.8}	-8.9		{+217.6}

^aFrom Ref. [13]

^cFrom Ref. [14]

^fFrom Ref. [15]

^gFrom Ref. [16]

^hFrom Ref. [17]

ⁱFrom Ref. [18]

^jFrom Ref. [19]

^kFrom Ref. [20].

the wave vector and n is the band index. Then we define the static self-energy as

$$\tilde{\Sigma}_{\mathbf{k}nn'} = \text{Re} \langle \psi_{\mathbf{k}n} | \frac{\Sigma(\epsilon_{\mathbf{k}n}) + \Sigma(\epsilon_{\mathbf{k}n'})}{2} | \psi_{\mathbf{k}n'} \rangle \quad (1)$$

where, $\epsilon_{\mathbf{k}n}$ denote eigenvalues, and Re means to take the hermitian part. By using this $\tilde{\Sigma}_{\mathbf{k}nn'}$ instead of the usual LDA exchange correlation potential $V_{\text{xc}}^{\text{LDA}}$, we can iterate to self-consistency, i.e. the $\tilde{\Sigma}_{\mathbf{k}nn'}$ generated by H_0 is identical to the $\Sigma_{\mathbf{k}nn'}$ that enters into H_0 . We explicitly include core contributions to Σ .

With the addition of local orbitals, we include in the MTO basis all atomic-like states that are within $\sim \pm 2$ Ry of the Fermi energy: thus both the 3d and 4d levels are included for GaAs, and so on. As QPscGW gives the self-consistent H_0 at the scalar relativistic level, we add the spin-orbit operator $H_{\text{SO}} = \vec{L} \cdot \vec{S}/2c^2$ to H_0 as a perturbation (it is not included in the self-consistency cycle). Thus the band structure is calculated from a one-body Hamiltonian $H_0 + H_{\text{SO}}$. We also considered a ‘scaled Σ ’

with

$$H_\alpha + H_{\text{SO}} = H_{\text{LDA}} + (1 - \alpha)(\tilde{\Sigma} - V_{\text{xc}}^{\text{LDA}}) + H_{\text{SO}}. \quad (2)$$

(Note that H_{LDA} and $V_{\text{xc}}^{\text{LDA}}$ are also determined from the self-consistent density given by H_0). Tables I and II present QPscGW results ($\alpha = 0$) for III-V and II-VI compounds. We also present results in a few cases where α is chosen to reproduce the experimental fundamental gap E_g at 0K, which we do to address the strong sensitivity of γ to E_g . The error in E_g from QPscGW theory, while small, is comparable to E_g itself for small-gap systems InAs and InSb, resulting in large errors in the effective mass m_c^Γ . Evidently once $(\tilde{\Sigma} - V_{\text{xc}}^{\text{LDA}})$ is scaled so E_g is reproduced, m_c^Γ falls in good agreement with the experimental mass. The magnitude of γ depends on the hybridization between the lower conduction band and the p -like conduction and valence bands. The hybridization depends on the position of the first two conduction band levels $E_0 = E(\Gamma_6^c) - E(\Gamma_8^v)$ and $E'_0 = E(\Gamma_7^c) - E(\Gamma_8^v)$. (In the absence of spin orbit coupling, Γ_6^c has Γ_1 symmetry; Γ_8^v, Γ_7^v and Γ_8^c, Γ_7^c are the valence and conduction levels

with Γ_{15} symmetry.) and is reflected in the magnitude of effective mass m_c^Γ . Also important is the strength of spin-orbit interaction at anion and cation sites, reflected in the spin orbit splittings Δ_{SO} and Δ'_{SO} of Γ_{15}^v and Γ_{15}^c . With the exceptions of Δ'_{SO} in InP and E_0 in AlP, all parameters are in good agreement with available experimental data. The experimental Δ'_{SO} seems low in InP and inconsistent with the trends described below. The discrepancy in E_0 for AlP is also curious as it falls well outside the error usually expected from QPscGW[2]; also its better known *fundamental* gap agrees well with QPscGW. It is likely that E_0 was misidentified in the (30 year old) experiment.

As the valence band has mostly anion character and the conduction band mostly cation character, one would expect that Δ_{SO} is controlled mainly by the anion, while Δ'_{SO} is controlled mainly by the cation. Comparing compounds with the same cation but different anions, or vice-versa, this trend becomes evident. For example, for GaP, GaAs and GaSb Δ'_{SO} is 0.158, 0.174, and 0.196 eV respectively; while on the other side for AlAs, GaAs and InAs Δ'_{SO} is 0.031, 0.174 and 0.429 eV. This trend is found in all materials presented in Tables I and II.

Fig. 1 shows the conduction band spin splitting versus wave number for the entire [110] line. For sufficiently small k it varies as k^3 as expected from the $\mathbf{k}\cdot\mathbf{p}$ analysis; γ was obtained by fitting a polynomial to the calculated splitting at k points near Γ . The sign of γ was determined from the eigenvectors and is defined according to the most accepted convention ($\Delta E = E(\Sigma_4) - E(\Sigma_3)$).

The splitting is rather complex, arising from several factors such as how the Γ_{15}^v and Γ_{15}^c states admix with the conduction state as k moves away from Γ . Still, inspection of Table 1 and Fig. 1 reveals some trends:

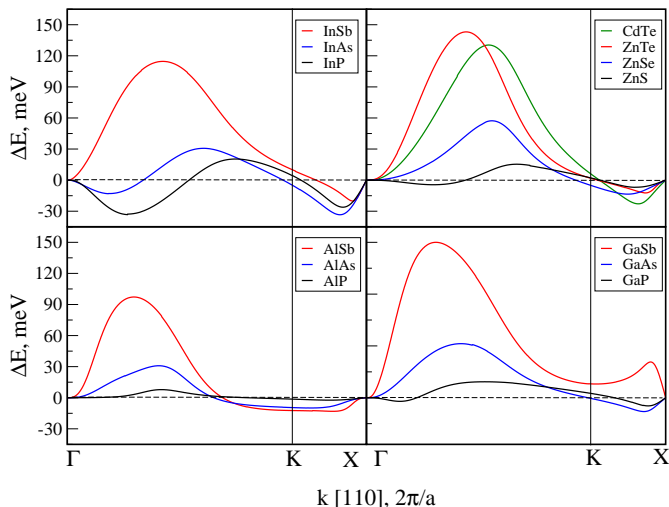


FIG. 1: Conduction band spin splitting in [110] direction. GaAs, GaSb, InP, InAs and InSb are plotted for the scaled Σ .

(i) γ scales approximately in proportion to $1/E_0$, at least in the narrow-gap case, as can be seen by comparing scaled ($H_\alpha + H_{SO}$) and unscaled ($H_0 + H_{SO}$) results for InAs and InSb. This is expected by the $\mathbf{k}\cdot\mathbf{p}$ theory. The scaling only slightly perturbs the potential; the band structure stays approximately constant except for small shifts in the lowest conduction band that substantially affect the gap and the conduction band shape near the Γ -point (and the valence band that couples to this band).

(ii) γ tends to increase as the spin-orbit coupling parameter $\Delta^- = 3 \langle (\frac{3}{2}\frac{3}{2})_v | H_{SO} | (\frac{3}{2}\frac{3}{2})_c \rangle$ becomes more negative. Δ^- becomes more negative with increasing anion mass, while the reverse is true when cation mass increases.

When anion mass increases, these tendencies add constructively and γ increases monotonically. When cation mass increases, these tendencies interfere with each other, and the behavior is more complex.

Table I compares our calculations of γ with the work of Cardona et al [12]. Those authors added empirical pseudo-Darwin potential shifts to make their band structure match the observed bandgap. These shifts result in a reasonable and qualitatively correct band structure, though band parameters have varying degrees of accuracy (e.g. m_c^Γ deviated from experiment as much as 35%[12]). The splittings we obtain are in qualitative, and often quantitative agreement with Cardona's calculations; e.g. ΔE changes sign at approximately the same k -points in GaP and GaAs.

What limited experimental data that exists is also shown in Table I. For GaAs [18], GaSb [19], InP [19], $|\gamma|$ was inferred from an estimation of the spin relaxation rate ascribed to the DP spin relaxation mechanism. This method does not resolve the sign of γ . For InSb γ was also extracted from electric-dipole-magnetic-dipole interference at far infrared frequencies [20], which is a more direct measure of the splitting and resolves the sign. This is probably the most accurate measurement of γ in any III-V semiconductor. The measurements of γ in Refs. [18, 19] are rather indirect and are based on extracting simultaneously and accurately spin and momentum relaxation times. Also there can be some uncertainty related to the type of momentum scattering mechanism.

Some care must be taken to determine γ in InSb. Owing to the small gap, the splitting begins to deviate from a k^3 dependence at very small k [21]. For the electron densities used in that work ($N_e = 1.6 \times 10^{14}$ to $4.7 \times 10^{15} \text{ cm}^{-3}$) the Fermi wave number k_F ranged between 0.9×10^{-3} and $2.7 \times 10^{-3} \text{ a.u.}^{-1}$. At this k , we find a small deviation from the k^3 dependence ($\sim 6\%$). However at larger doping the renormalization is significant: at $k = 10 \times 10^{-3} \text{ a.u.}^{-1}$ the splitting is reduced by 40% (i.e. $\Delta E/\gamma k^3 = 0.6$) in InSb, by 20% in InAs, but is negligible in the remaining semiconductors.

In Fig. 2 we show the LDA and QPscGW spin splitting together with the corresponding bands for GaAs.

TABLE II: Important band parameters for the II-VI semiconductors. Symbols are the same as in Table I. Experimental data are taken from Ref. 13 unless noted otherwise.

	ZnS	ZnSe	ZnTe	CdTe
E_0	4.00	2.94	2.45	1.84
(expt)	(3.78)	(2.82)	(2.394)	(1.606)
$E'_0 - E_0$	4.59	4.52	2.91	3.57
Δ_{SO}	0.084	0.408	0.884	0.829
(expt)	(0.065) ^a	(0.4)	(0.91)	(0.81) ^a
Δ'_{SO}	0.140	0.133	0.110	0.305
Δ^-	+0.16	-0.15	-0.44	-0.28
m_c^Γ	0.186	0.131	0.113	0.100
(expt)	(0.184)	(0.13)	(0.13)	(0.096) ^b
γ	-0.48	+1.29	+13.3	+8.5
{Ref. 12}		{+1.6}		{+11.7}

^aFrom Ref. [16]

^bFrom Ref. [22]

Roughly speaking, the spin splitting of the lowest conduction band is induced by hybridization with the cation-like conduction band and the anion-like valence bands of p symmetry. These two bands contribute to γ with opposite sign. Dispersion in the relevant bands on the [110] line differs significantly in the LDA from the QPsc GW case; but the relative difference is largest near Γ point where the LDA overestimates the sp hybridization. Consequently the relative difference in LDA and QPsc GW conduction band spin splitting is largest near Γ : γ^{LDA} is +121 eV·Å³ in GaAs, which is very different from the 6.4 or 8.5 eV·Å³ in Table I. Near X where the splitting is linear in k , LDA and QPsc GW splittings are very similar. This trend is common to all materials tested.

Until now, several authors have relied on the $\mathbf{k}\cdot\mathbf{p}$ ap-

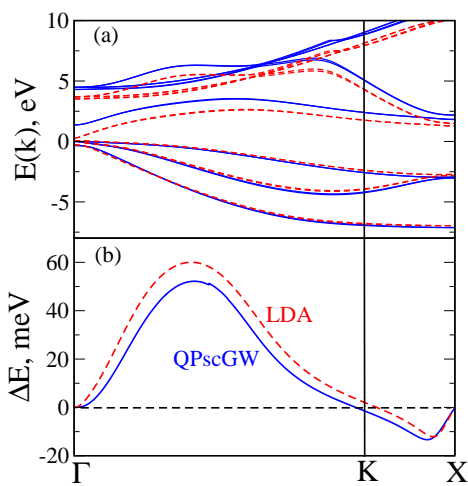


FIG. 2: (a) The LDA (red dashed line) and QPsc GW (solid blue line) upper valence and lower conduction bands. (b) The LDA (red dashed line) and QPsc GW (solid blue line) conduction bands spin splitting in [110] direction.

proximation to estimate the value of γ [12, 21, 23]. Generally speaking, the “downfolded” $\mathbf{k}\cdot\mathbf{p}$ Hamiltonian (i.e. with the far band contributions folded in) can contain all possible independent parameters consistent with the crystal symmetry at the Γ point. However, it is not possible to determine these parameters just from experiments. Thus it is necessary to assume a number of constraints so as to reduce the number of the parameters. For example, a usual approximation is that the Luttinger’s “residual γ parameters” for the unoccupied p bands are taken to be zero [23]. However, constraints vary from paper to paper [12, 23], and the spin splitting one obtains depends on the choice of constraint. In principle, all parameters can be calculated from the GW hamiltonian without making any additional assumptions, in which case the downfolded Hamiltonian should reproduce all the GW QP levels exactly near Γ . However, the parametrization of $\mathbf{k}\cdot\mathbf{p}$ theory is based on the Luttinger-Kohn expansion of the $\psi_{\mathbf{k}n}$ [24], where the periodic part of $\psi_{\mathbf{k}n}$ at $\mathbf{k} \neq 0$ is expanded by ψ_{0n} . This is neither convenient nor suitable for the parametrization of *ab initio* eigenfunctions. It is on the other hand rather straightforward to expand all the required matrix elements in the basis of the *ab initio* $\psi_{\mathbf{k}n}$ that respect the crystal symmetry.

In conclusion, we employed a recently developed QPsc GW to make *ab initio* predictions of the conduction band spin splitting in III-V and II-VI semiconductors. (In a few cases, a small empirical adjustment to the self-energy was also needed.) Such an approach is essential to reliably determine the splitting; moreover it builds a framework that will enable builders of model hamiltonians to reliably incorporate the effect without the need for additional assumptions.

The authors gratefully acknowledge support from the Office of Naval Research. A. N. Chantis is thankful to X. Cartoixà and D. Z.-Y. Ting for fruitful scientific discussions.

- [1] S. Faleev, M. V. Schilfgaarde, and T. Kotani, Phys. Rev. Lett. **93**, 126406 (2004).
- [2] M. V. Schilfgaarde, T. Kotani, and S. Faleev, cond-mat/0510408 (2005).
- [3] M. V. Schilfgaarde, T. Kotani, and S. Faleev, cond-mat/0508295 (2005).
- [4] G. Dresselhaus, Phys. Rev. **100**, 580 (1955).
- [5] G. E. Pikus and A. N. Titkov, in *Optical Orientation*, edited by F. Meier and B. P. Zakharchenya (North-Holland, Amsterdam, 1984).
- [6] Y. A. Bychkov and E. I. Rashba, J. Phys. C: Solid State Phys. **17**, 6039 (1984).
- [7] M. I. Dyakonov and V. Y. Kachorovskii, Sov. Phys. Semicond. **20**, 110 (1986).
- [8] N. S. Averkiev and L. E. Golub, Phys. Rev. B **60**, 15582 (1999).
- [9] X. Cartoixà, D. Z.-Y. Ting, and Y.-C. Chang, Phys. Rev.

B **71**, 045313 (2005).

[10] W. Knap, C. Skierbiszewski, A. Zduniak, E. Litwin-Staszewska, D. Bertho, F. Kobbi, J. L. Robert, G. E. Pikus, F. G. Pikus, S. V. Iordanskii, et al., Phys. Rev. B **53**, 3912 (1996).

[11] B. Jusserand, D. Richards, G. Allan, C. Priester, and B. Etienne, Phys. Rev. B **51**, 4707 (1995).

[12] M. Cardona, N. E. Christensen, and G. Fasol, Phys. Rev. B **38**, 1806 (1988).

[13] O. Madelung, *Semiconductors Basic Data* (Springer-Verlag, Berlin, 1996).

[14] D. F. Nelson, L. F. Johnson, and M. Gershenzon, Phys. Rev. **135**, A1399 (1964).

[15] A. V. Varfolomeeve, R. P. Seisyan, and R. N. Yokimova, Sov. Phys. Semicond. **9**, 530 (1975).

[16] O. Madelung, M. Schulz, and H. Weis, eds., *Landolt-Börnstein: Numerical Data and Functional Relationships in Science and Technology*, vol. III/17a,b (Springer-Verlag, Berlin, 1982).

[17] C. Jung and P. R. Bressler, J. Elec. Spec. and Rel. Phenom.. **78**, 503 (1996).

[18] V. A. Marushchak, M. N. Stepanova, and A. N. Titkov, Fiz. Tverdogo Tela **25**, 1170 (1983).

[19] A. T. Gorelenok, V. A. Marushchak, and A. N. Titkov, Izv. Akad. Nauk SSSR, Ser. Fiz. **50**, 290 (1986).

[20] Y.-F. Chen, M. Dobrowolska, J. K. Furdyna, and S. Rodriguez, Phys. Rev. B **32**, 890 (1985).

[21] G. E. Pikus, V. A. Marushchak, and A. N. Titkov, Sov. Phys. Semicond. **22**, 115 (1988).

[22] K. K. Kanazawa and F. C. Brown, Phys. Rev. **135**, A1757 (1964).

[23] P. Pfeffer and W. Zawadzki, Phys. Rev. B **53**, 12813 (1996).

[24] J. M. Luttinger and W. Kohn, Phys. Rev. B **97**, 869 (1954).